eXPRESS Polymer Letters Vol.8, No.6 (2014) 425–435
Available online at www.expresspolymlett.com
DOI: 10.3144/expresspolymlett.2014.46

Study on the structure-properties relationship of natural rubber/SiO_2 composites modified by a novel multi-functional rubber agent

S. Y. Yang[1], *L. Liu*[2], *Z. X. Jia*[2*], *W. W. Fu*[2], *D. M. Jia*[2], *Y. F. Luo*[2]

[1]Chemical Industrial Cleaner Production and Green Chemical R&D Center of Guang Dong Universities, Dongguan University of Technology, Dongguan, China
[2]College of materials science and engineering, South China University of Technology, Guangzhou, China

Received 13 December 2014; accepted in revised form 9 February 2014

Abstract. Vulcanization property and structure-properties relationship of natural rubber (NR)/silica (SiO_2) composites modified by a novel multi-functional rubber agent, N-phenyl- N′-(γ-triethoxysilane)-propyl thiourea (STU), are investigated in detail. Results from the infrared spectroscopy (IR) and X-ray photoelectron spectroscopy (XPS) show that STU can graft to the surface of SiO_2 under heating, resulting in a fine-dispersed structure in the rubber matrix without the connectivity of SiO_2 particles as revealed by transmission electron microscopy (TEM). This modification effect reduces the block vulcanization effect of SiO_2 for NR/SiO_2/STU compounds under vulcanization process evidently. The 400% modulus and tensile strength of NR/SiO_2/STU composites are much higher than that of NR/SiO2/TU composites, although the crystal index at the stretching ratio of 4 and crosslinking densities of NR/SiO_2 composites are almost the same at the same dosage of SiO_2. Consequently, a structure-property relationship of NR/SiO_2/STU composites is proposed that the silane chain of STU can entangle with NR molecular chains to form an interfacial region, which is in accordance with the experimental observations quite well.

Keywords: *rubber, multi-functional rubber agent, structure-property relationship, silica*

1. Introduction

In recent years, polymer/inorganic filler composites have attracted great attention, not only in industry, but also in academia, for inorganic filler, such as silica (SiO_2), montmorillonite and halloysite nanotube can introduce great improvement in the mechanical properties of polymer/inorganic filler composites even at low dosage of filler [1]. Among these fillers, silica is believed to be one of the most important inorganic fillers applied to reinforce rubber vulcanizates because the compounding of silica offers a number of advantages on the mechanical properties of vulcanizates, such as excellent thermal stability, tensile strength, good tear and abrasion resistance [2, 3]. However, because of great discrepancies in polarity between the non-polar diene polymer and polar silica, primary particles of SiO_2 tend to aggregate due to the thermo-dynamical incompatibility driving force caused by hydrogen bonds among primary particles [4, 5]. Research revealed that on a larger scale, up to macroscopic scale, the silica spatial distribution is homogeneous, with no sign of connectivity at 5% and with connectivity at 15% [6].

On the other hand, except for the well dispersion of SiO_2 particles, the interfacial adhesion between polymer matrix and SiO_2 particles is another essential factor for the mechanical properties of compos-

*Corresponding author, e-mail: zxjia@scut.edu.cn

ites [7], as the weak interfacial adhesion would cause catastrophic damages to the matrix under applied stress. Thus, improvements in the interfacial adhesion between the two phases, as well as good dispersion of inorganic filler particles, have been realized in the preparation of polymer-filler hybrid composites using coupling agents [8]. Nakamura *et al*. [9] investigated the effect of the number of siloxane units on the mechanical properties of polyisoprene/SiO_2 composites by using silanes with dialkoxy and trialkoxy structures. The reinforcement effect introduced by the silane treatment of silica was found depend strongly both on the entanglement between the silane chain and polyisoprene rubber matrix and on the crosslinking reaction between the mercapto group of silane and polyisoprene rubber in the interfacial region, which is in accordance with results from other researches [7]. However, silane coupling agents can only modify the surface of SiO_2, promoting a good dispersion of SiO_2 in the rubber matrix. It has been realized that, except for the fine-dispersion of filler in rubber matrix, if the silane coupling agents possess another function of rubber agents, like acceleration function, the properties of rubber composites will be significantly promoted [8].

Moreover, binary accelerator systems are being widely applied in the rubber industry and become increasingly popular based on the fact that such binary systems can effectively facilitate the vulcanization process to be carried out at a lower temperature within a short time [10–12]. Among these binary accelerator systems, thiourea (TU) and its derivatives are favorable for improvements in the vulcanization process and mechanical properties of rubber composites [13, 14]. Kurien and Kuriakose [15] synthesized a sort of TU derivative, namely amidino thiourea (ATU), and studied the vulcanization properties of NR with binary accelerator systems including tetramethylthiuram disulphide (TMTD), mercapto-benzothiazyl disulphide (MBTS), or cyclohexyl-benzthiazyl-sulphenamide (CBS). The induction time and optimum curing time of the formulations with ATU or TU were shorter than that of the control references without ATU or TU. However, all these TU derivatives only can accelerate the vulcanization process of rubber composites. Consequently, how to combine the accelerating property of TU and surface modification function of coupling agent together still attracted great attentions both in academy and in industry.

In this work, a multi-functional rubber agent, N-phenyl-N′-(γ-triethoxysilane)-propyl thiourea (STU), was used to prepare NR/SiO_2 composites and the vulcanization property, as well as structure-properties relationship, was investigated in detail.

2. Experimental

2.1. Materials

Natural rubber ISNR-3 was used, and the other ingredients, such as zinc oxide (ZnO), stearic acid (SA), N-cyclohexyl-2-benzothiazole sulfonamide (CBS), thiourea (TU) and sulfur (S) were commercial grades. Precipitated silica (SiO_2), with the particle diameter of about 900 nm and BET surface area of 144.44 m^2/g, was kindly supplied by Huiming Chemical Industry Co. Ltd, Wanzai County, China. The synthesis of STU was performed by mixing γ-aminopropyl triethoxysilane and phenyl isothiocyanate drop by drop in a stoichiometric level under the room temperature for 24 hours. The details in FTIR and ^{1}H-NMR of STU are given as follow:

FTIR, cm^{-1} (neat): 3275br, (ν_{NH}); 3060w, (ν_{CH}, arom.); 2974m, 2927m, 2887m (ν_{CH}, alif.); 1597m (phenyl); 1536s (ν_{CNC}, B-band); 1450m ($\nu_{C–C}$, arom.); 1165m ($\nu_{C=S}$); 1078s ($\nu_{Si–O–Et}$) [16–18].

^{1}H-NMR, δ ($CDCl_3$): 8.14 (w, 1H, N′H); 7.37 (m, 2H, $H_{m,m'}$); 7.26 (m, 1H, H_p); 7.18 (m, 2H, $H_{o,o'}$); 6.25 (w, 1H, NH); 3.73 (s, 6H, ethoxy CH_2); 3.61 (m, 2H, γ-CH_2); 1.68 (m, 2H,β-CH_2); 1.13 (s, 9H, ethoxy CH_3); and 0.55 (m, 2H, α-CH_2). The chemistry structure of STU is displayed in Figure 1.

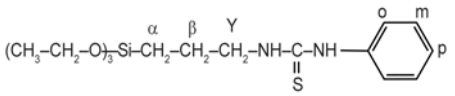

Figure 1. The chemistry structure of STU

2.2. Preparation of NR/SiO_2 compounds

The formulations of NR/SiO_2 compounds are summarized in Table 1 and Table 2.

NR was passed through the roller three times on an open two-roll mill (160 mm×320 mm) at room temperature with the nip gap of about 1 mm, then other ingredients, such as SiO_2, ZnO, SA, TU or STU, CBS and sulfur, were added to the glue stock one by one within ten minutes. After that, the compounds were stored for eight hours before the rheometer testing.

Table 1. The formulation of NR/SiO_2/STU composites [phr]

Sample	NR	STU	ZnO	SA	CBS	S	SiO_2
STU-SiO_2-0	100.0	0.92	5.0	2.0	2.64	1.5	0.0
STU-SiO_2-10	100.0	0.92	5.0	2.0	2.64	1.5	10.0
STU-SiO_2-20	100.0	0.92	5.0	2.0	2.64	1.5	20.0
STU-SiO_2-30	100.0	0.92	5.0	2.0	2.64	1.5	30.0
STU-SiO_2-40	100.0	0.92	5.0	2.0	2.64	1.5	40.0
STU-SiO_2-50	100.0	0.92	5.0	2.0	2.64	1.5	50.0

Table 2. The formulation of NR/SiO_2/TU composites [phr]

Sample	NR	TU	ZnO	SA	CBS	S	SiO_2
TU-SiO_2-0	100.0	0.20	5.0	2.0	2.64	1.5	0.0
TU-SiO_2-10	100.0	0.20	5.0	2.0	2.64	1.5	10.0
TU-SiO_2-20	100.0	0.20	5.0	2.0	2.64	1.5	20.0
TU-SiO_2-30	100.0	0.20	5.0	2.0	2.64	1.5	30.0
TU-SiO_2-40	100.0	0.20	5.0	2.0	2.64	1.5	40.0
TU-SiO_2-50	100.0	0.20	5.0	2.0	2.64	1.5	50.0

2.3. Characterization

The vulcanization research was carried out by a MDR (UR-2030SD, U-Can Limited Corporation, Taiwan, China) at 133°C. The compounds were cured at 133°C according to their optimum vulcanization time. The mechanical properties, such as 400% modulus, tensile strength, and elongation at break, were measured according to ISO/DIS37-1994 specifications. U-CAN electron tensile testing machine was used with the crosshead speed of 500 mm/min. All mechanical testing was undertaken at 25°C.

The possible chemical interactions between STU and SiO_2 were probed by infrared spectroscopy (IR) and X-ray photoelectron spectroscopy (XPS). For preparation of samples, SiO_2 and STU/SiO_2 (0.92/30, phr) model compounds were placed on a vulcanizing press machine at a setting time of 15 min under 133°C, followed by Soxhlet extraction experiment of the model compounds using boiling benzene (100°C) within 24 h, and then were dried to constant weight. The IR measurement of model compounds was recorded on a Bruker Vector 33 infrared spectroscopy in the range of 4000~400 cm^{-1}. Also, XPS spectra of the model compounds were recorded by using an X-ray photoelectron spectrometer (Kratos Axis Ultra DLD) with an aluminum (mono) K_α source (1486.6 eV). The aluminum K_α source was operated at 15 kV and 10 mA. All core level spectra were referenced to the C_{1s} neutral carbon peak at 284.7 eV.

The crosslinking density [19] test was performed on the base of swelling equilibrium measurement. The swelling equilibrium test was carried out by immersing samples in the toluene for 4 days. After that, the surface toluene was blotted off quickly with tissue paper. The specimens were immediately weighed on an analytical balance and then dried in a vacuum oven until the samples became constant weight and reweighed. The calculation was made according to the reference [20].

For the observation by transmission electron microscopy (TEM), the specimens were ultramicrotomed into thin pieces of about 100 nm in thickness with Leica EMUC6 under liquid nitrogen atmosphere. Then the observations were obtained using a Tecnai 12 transmission electron microscope (FEI Company, Holland) with an accelerating voltage of 100 kV.

The strain-induced crystallization (SIC) of NR/SiO_2 composites was performed on a WAXD apparatus (Philips X′ Pert PRO, Holland) with Ni-filtered Cu K_α radiation($\lambda = 0.154$ nm) at a generator voltage of 40 kV and generator current of 40 mA. The 2θ scanning rang was varied from 5 to 30°, with a step of 0.017° and a measuring time of 16.24 s per step. The degree of SIC (X_c) is calculated on the basis of peaks fitting during which a 2θ range from 10 to 30°, including crystalline and amorphous, was taken. X_c is defined as the ratio between the single integrated intensity of crystal (200 or 120 reflection was taken) A_c and the total integrated intensity of crystalline

and amorphous peaks A_{c+a} in the 2θ range, as expressed in the following Equation (1):

$$X_c = \frac{A_c}{A_{c+a}} \times 100\% \quad (1)$$

3. Results and discussions

3.1. Characterization of model compounds

3.1.1. IR spectroscopy

Figure 2 shows the IR spectra of SiO_2 and STU/SiO_2 model compounds. The peaks at 3441 and 1103 cm^{-1} are assigned to the stretching vibrations of –OH groups on the surface of SiO_2 and Si–O groups, respectively. In the spectrum of STU/SiO_2 model compounds, the stretching vibration of Si–O groups does not change, whereas the peak at 3423 cm^{-1} is associated with the stretching vibration of –NH groups with the bending vibration at 1550 cm^{-1}. Two reasons may be responsible for the unconspicuous representation of –OH groups. First, partial hydroxyl groups have reacted with the siloxane groups of STU, leading to a decrease in the amount of –OH groups. Second, the silane molecules have grafted to SiO_2 particles and covered on the surface of SiO_2 particles, which would give rise to the shielding effect for –OH groups. In the dotted line ellipse domain, the peaks located at 2983 and 2945 cm^{-1} are ascribed to stretching vibrations of methyl and methylene. Moreover, the characteristic stretching vibrations of benzene ring (1597 cm^{-1}) and C=S (1165 cm^{-1}) have disappeared, illuminating that a pyrolysis reaction of STU occurs during heating press [21].

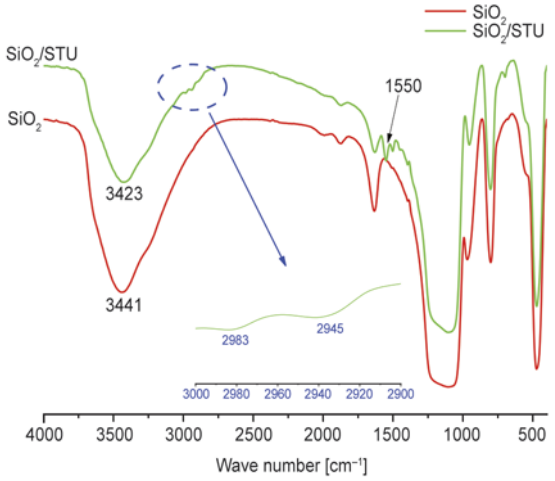

Figure 2. The IR spectra of SiO_2 and STU/SiO_2 model compounds

3.1.2. XPS analysis

In order to substantiate the formation of chemical bonds between SiO_2 and STU, XPS survey was performed on the model compounds. The formation of

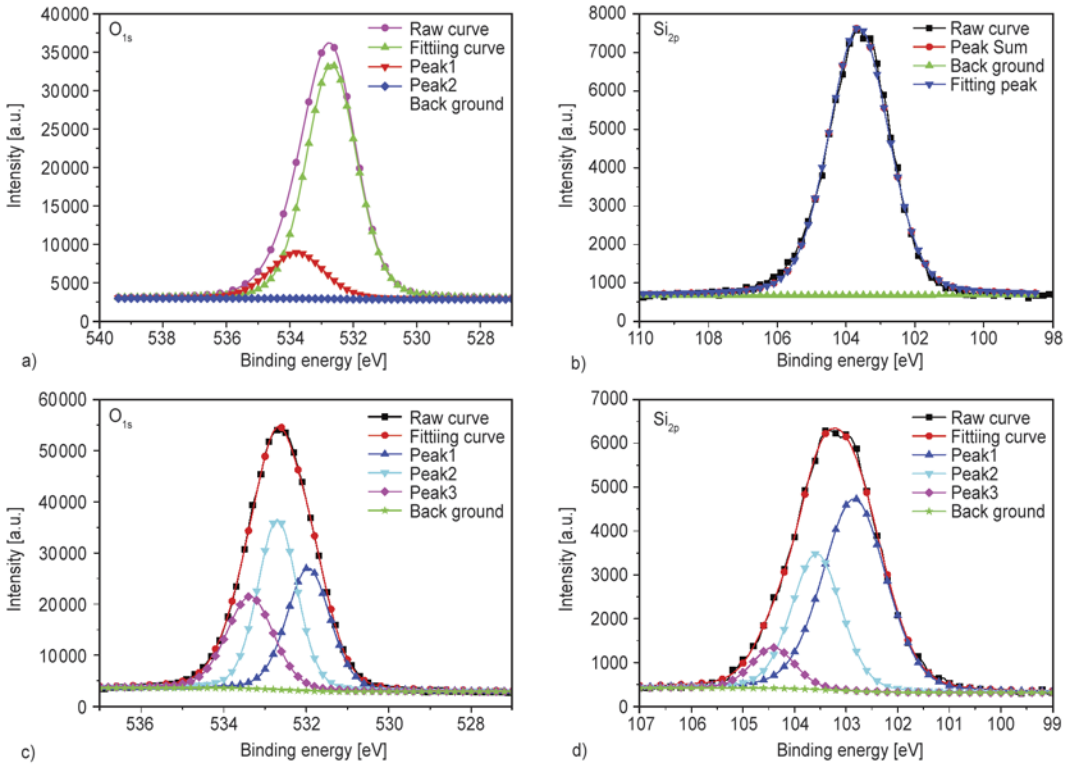

Figure 3. The XPS fitting peaks of model compounds: a) O_{1s} and b) Si_{2p} of SiO_2; c) O_{1s} and d) Si_{2p} of STU/SiO_2

Table 3. The characteristic parameters of fitting peaks of model compounds SiO_2 and STU/SiO_2

Sample	Si_{2p}			O_{1s}		
SiO_2	–	103.6	–	–	532.7	533.8
STU/SiO_2	102.8	103.6	104.4	532.0	532.7	533.4

chemical bond will cause a variation in the binding energies of certain atoms related to the chemical bond. The XPS spectra of SiO_2 and STU/SiO_2 model compounds are depicted in Figure 3 and Table 3. The characteristic signal due to silicon (Si_{2p} at 103.6 eV) of SiO_2 is detected, meanwhile, that for STU/SiO_2 model compounds is split into three characteristic signals, 102.8, 103.6 and 104.4 eV, respectively, indicating two new different chemical environments of silicon atom have been introduced to the surface of SiO_2. Moreover, one can see that there are two different binding energies, 532.7 and 533.8 eV, of O_{1s} in pure SiO_2, whereas, three evident peaks are found in the O_{1s} spectra of STU/SiO_2 model compounds, confirming the successful modification of SiO_2 particles by STU, as shows in Figure 4. The silanol groups of STU can react with the hydroxyl groups on the surface of SiO_2 with the elimination of ethanol [8] and phenyl isothiocyanate molecules under heating. The modification of SiO_2 will further prohibit the agglomeration of SiO_2 particles, as well as the physical adsorption of SiO_2 to rubber agents.

3.2. Vulcanization property of NR/SiO_2 compounds

The vulcanization parameters of NR/SiO_2/TU compounds and NR/SiO_2/STU compounds are showed in Table 4 and Table 5, separately. In Table 4, the scorch time (T_{s1}) and optimum curing time (T_{c90}) increase with increasing SiO_2, even at low SiO_2 dosage, indicating that SiO_2 particles can delay the vulcanization process. From the lowest torque (*ML*), *ML* value, as well as the *MH* value, dramatically change with the incorporation of SiO_2, elucidating a bad dispersion of SiO_2, that is, particles connectivity, in the NR matrix. In Table 5, the scorch time (T_{s1}) and optimum curing time (T_{c90}) also increase with increasing SiO_2, however, compared with NR/SiO_2/TU compounds, one can see that a

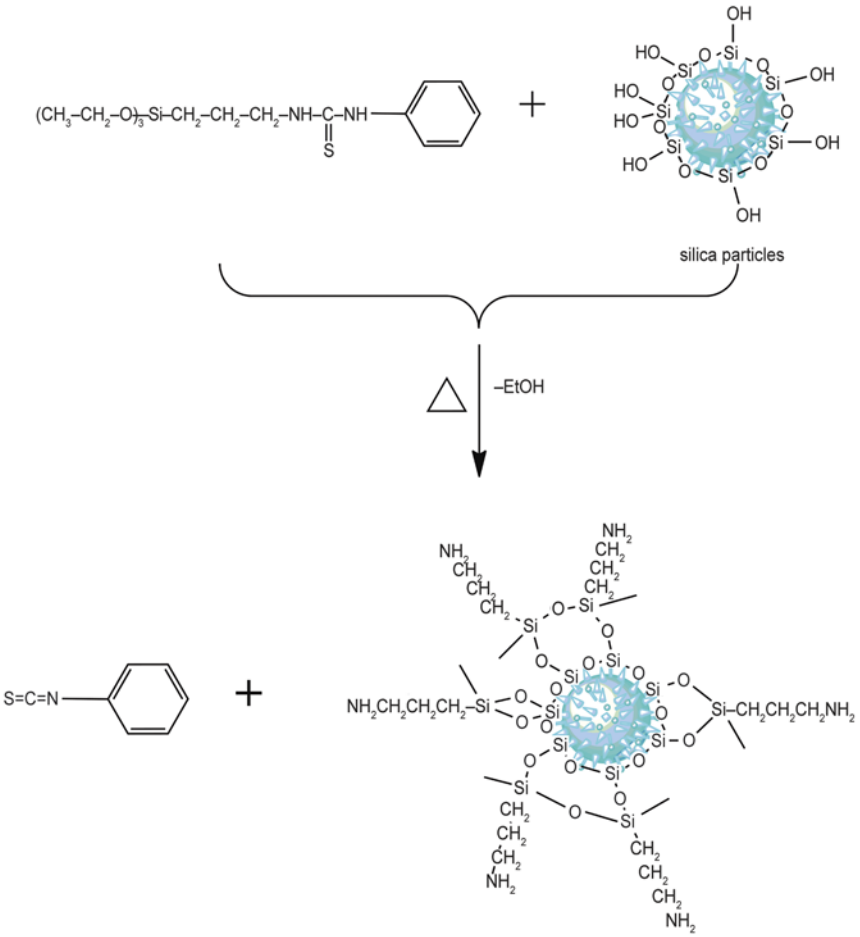

Figure 4. Schematic of STU modified silica particles

Table 4. The curing characteristics of NR/SiO_2/TU compounds (133°C)

Sample	T_{s1} [min]	T_{c90} [min]	ML [dN·m]	MH [dN·m]
TU-SiO_2-0	1.68	6.77	0.08	13.71
TU-SiO_2-10	5.30	11.10	0.28	15.15
TU-SiO_2-20	8.68	16.13	0.39	17.30
TU-SiO_2-30	8.90	17.78	1.16	22.60
TU-SiO_2-40	6.98	18.27	2.79	28.37
TU-SiO_2-50	9.03	28.27	4.08	31.07

Table 5. The curing characteristics of NR/SiO_2/STU compounds (133°C)

Sample	T_{s1} [min]	T_{c90} [min]	ML [dN·m]	MH [dN·m]
STU-SiO_2-0	3.10	8.15	0.05	13.20
STU-SiO_2-10	4.75	9.81	0.10	14.43
STU-SiO_2-20	5.63	10.97	0.10	14.97
STU-SiO_2-30	6.97	13.52	0.30	18.97
STU-SiO_2-40	8.27	18.85	1.75	26.27
STU-SiO_2-50	9.53	26.53	5.21	32.66

more moderate increase in the NR/SiO_2/STU compounds, suggesting a lower physical adsorption of SiO_2 particles to rubber agents. Meanwhile, when the incorporation of SiO_2 is lower than 30 phr, the *ML* or *MH* of NR/SiO_2/STU compounds evolves to high value slightly, which is quite different from NR/SiO_2/TU compounds. This can be attributed to the modified effect of STU.

3.3. Morphology of NR/SiO_2 composites

TEM technology is competent for analyzing the dispersed morphology of SiO_2 particles in the rubber matrix. Figure 5 is the TEM graphs of STU-SiO_2-30 vulcanizate (a) and TU-SiO_2-30 vulcanizate (b). As is readily seen, a result can be expected that the dispersion degree of Figure 5a seems to be more homogeneous than Figure 5b, which suggests that STU facilitates SiO_2 particles to disperse in NR matrix uniformly. In Figure 5a, the size of silica aggregation is reduced to a certain extent and not evident connectivity of SiO_2 particles is found, that is, the SiO_2 particles aggregations have been isolated by NR rubber matrix due to the modified effect of STU, as depicts in Figure 4. However, in Figure 5b, an opposite phenomenon is observed that SiO_2 particles trend to agglomerate seriously and the connectivity between particles has been formed, which can be assigned to the formation of hydrogen bonds among SiO_2 particles by thermodynamical driving force [7] and the huge difference in compatibility between silica particles and NR matrix.

3.4. Strain-induced crystallization (SIC) of NR/SiO_2 composites

It has been recognized long ago that the excellent tensile property of NR originates from SIC. The details of strain-induced crystallization of NR/SiO_2

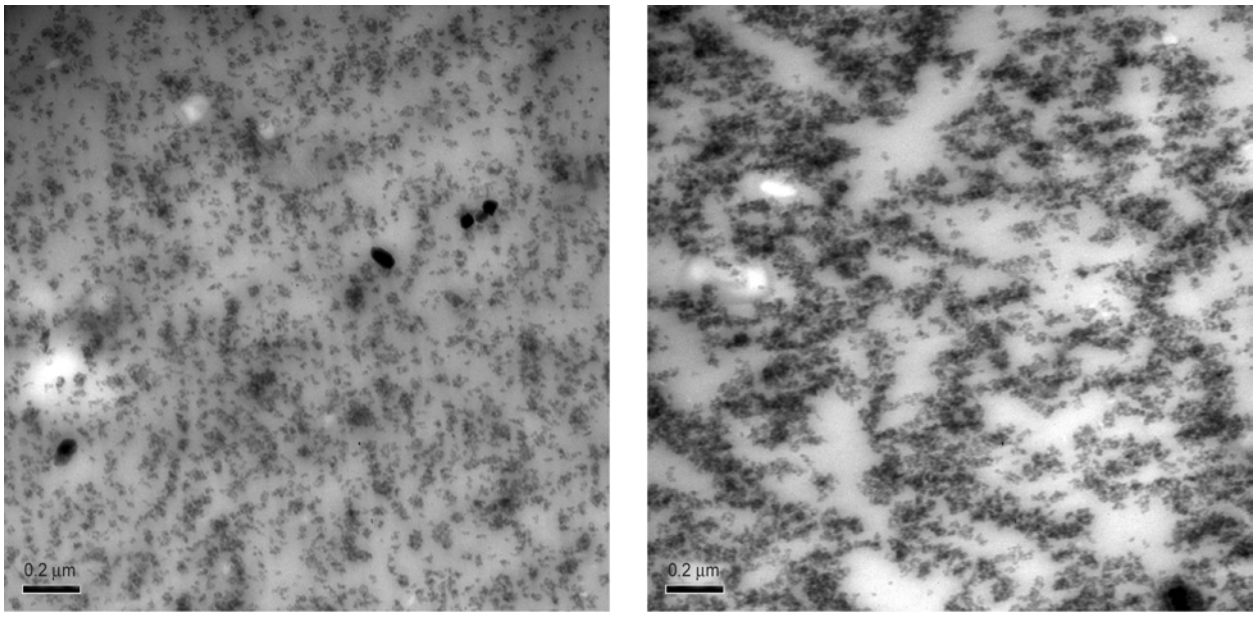

a) b)

Figure 5. The TEM photographs of STU-SiO_2-30 vulcanizate (a) and TU-SiO_2-30 vulcanizate (b)

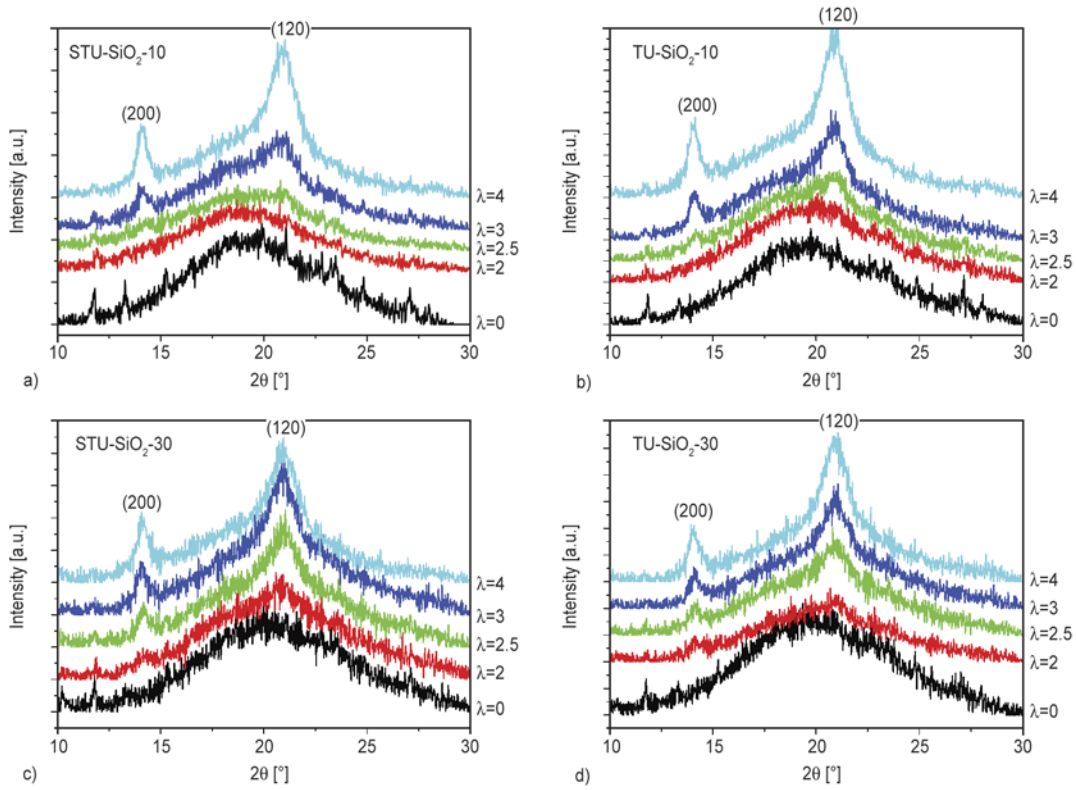

Figure 6. Equatorial diffraction profiles at selected strain values of vulcanizates as a function of strain under stretching at the 2θ angle range of 5–30°: STU-SiO_2-10 vulcanizate (a), TU-SiO_2-10 vulcanizate (b), STU-SiO_2-30 vulcanizate (c) and TU-SiO_2-30 vulcanizate (d)

composites experiments have been expressed in section 2.3. and the crystal index (CI) is calculated according to Equation (1). In this section, four NR/SiO_2 composites, STU-SiO_2-10, STU-SiO_2-30, TU-SiO_2-10 and TU-SiO_2-30, is adopted to illuminate the SIC of NR/SiO_2 composites according to the dispersion state of SiO_2 in the NR matrix. The diffraction profiles of STU-SiO_2-10, STU-SiO_2-30, TU-SiO_2-10 and TU-SiO_2-30 under different ratio at the 2θ angle range of 5–30° are shown in Figure 6, indicating that NR is a typical strain-induced crystallization material. Figure 7 illuminates the strain dependence of CI of NR/SiO_2 composites. In Figure 7a, when the stretching ratio is lower than 2.5,

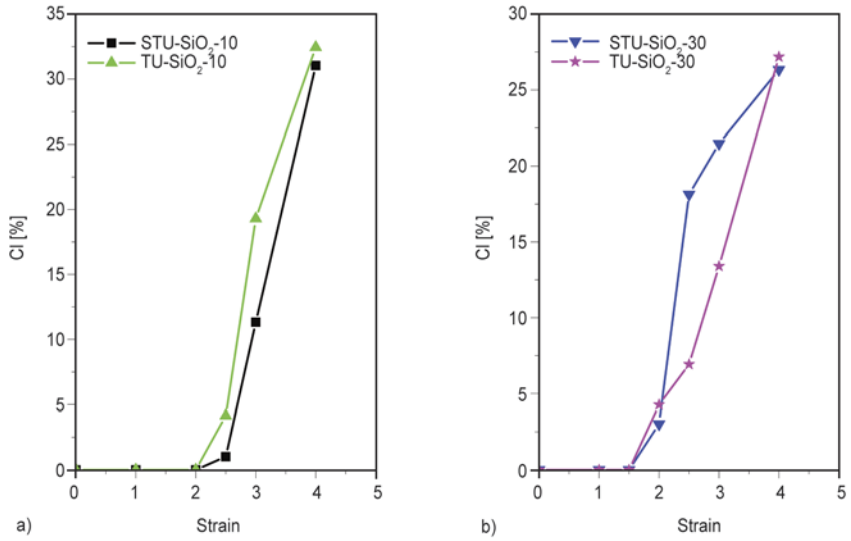

Figure 7. Variation of CI of NR with different vulcanization systems during the stretching process: filler content at 10 phr (a) and filler content at 30 phr (b)

not crystallization can be observed in STU-SiO_2-10 and TU-SiO_2-10 composites. After that, a steep upturning appears, indicating the orientated NR molecules begin to crystallize. The SIC rate of TU-SiO_2-10 is higher than that of STU-SiO_2-10, however, as the stretching ratio reaches 4, the CI is not apparent difference between STU-SiO_2-10 and TU-SiO_2-10. As one can see in Figure 7b, the initial crystallization strains of STU-SiO_2-30 and TU-SiO_2-30 are at the stretching ratio of 2, suggesting the incorporation of SiO_2 induces the NR molecules to crystallize. With respect to Figure 7a, the SIC rate of STU-SiO_2-30 increases faster than that of TU-SiO_2-30 at the stretching ratio of 2~3, illustrating the rubber molecules in STU-SiO_2-30 are readily to orientate. At the stretching ratio of 4, the CI is almost the same between STU-SiO_2-30 and TU-SiO_2-30.

3.5. Structure-property relationship of NR/SiO_2 composites

The stress-strain behavior of NR/SiO_2 composites is displayed in Figure 8 and Table 6. Compared the difference between *ML* and *MH* ($\Delta M = MH - ML$) in Table 4 and 5 with the crosslinking densities in Table 6 for NR/SiO_2 composites, the discrepancy between ΔM and crosslinking density is mainly attributed to the hydrodynamic volume effect of filler and the hardness discrepancy between filler and rubber [22]. In the NR/SiO_2/STU composites, the tensile strength increases with increasing SiO_2. As the addition of SiO_2 reaches 30 phr, the maximum tensile strength is about 30.75 MPa, following by a decrease in the tensile strength with increasing SiO_2, which is the same trend for NR/SiO_2/TU composites. However, the maximum tensile strength for NR/SiO_2/TU composites is only 25.52 MPa at the SiO_2 content of 30 phr, which is much lower than that of NR/SiO_2/STU composites. As is shown in Figure 7, the CI of NR/SiO_2 composites are almost the same at the stretching ratio of 4, so in this work, for distinct understanding of the enhancement of STU, 400% modulus of NR/SiO_2 composites is acquired, rather than 100 and 300% modulus. 400% modulus of NR/SiO_2/STU composites is higher than that of NR/SiO_2/TU composites at the same addition of SiO_2, suggesting that the reinforcing mechanism of NR/SiO_2/STU composites is quite different from NR/SiO_2/TU composites.

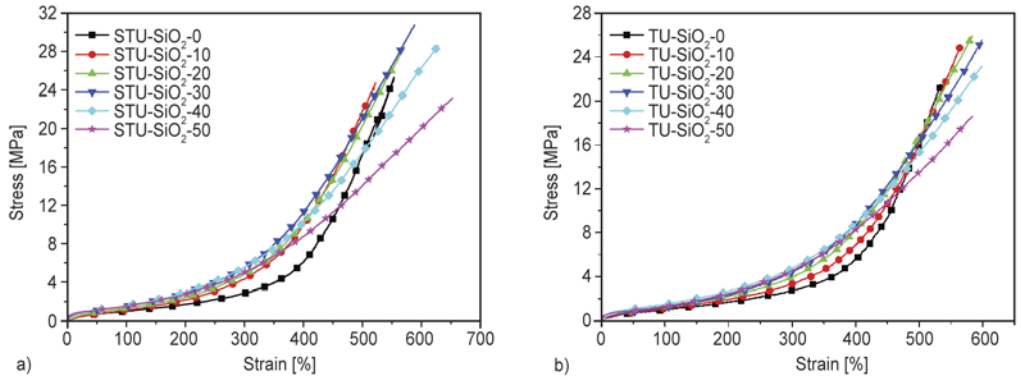

Figure 8. The stress-strain behavior of NR/SiO_2/STU composites (a) and NR/SiO_2/TU composites (b)

Table 6. The mechanical performance of NR/SiO_2 composites

Sample	400% Modulus [MPa]	Tensile-strength [MPa]	Elongation at break [%]	V_e [10^{-4}]
STU-SiO_2-0	6.08	25.29	553	1.2290
STU-SiO_2-10	9.94	24.74	522	1.2180
STU-SiO_2-20	10.14	28.35	573	1.0540
STU-SiO_2-30	11.26	30.75	609	0.9768
STU-SiO_2-40	10.25	28.36	627	0.8505
STU-SiO_2-50	8.73	23.11	646	0.5979
TU-SiO_2-0	5.53	21.49	534	1.2050
TU-SiO_2-10	6.84	24.71	578	1.1140
TU-SiO_2-20	8.27	25.09	584	1.0180
TU-SiO_2-30	8.79	25.52	602	0.8608
TU-SiO_2-40	8.81	22.95	599	0.7152
TU-SiO_2-50	8.29	18.07	592	0.5148

It is well known that the stress-strain behavior for filler filled rubber systems is affected by the crosslinking density [23], the size of agglomerates formed by filler [24], rubber/filler interactions [7, 23] and CI (only for crystal polymer) of rubber matrix. In Table 6 and Figure 7, the crosslinking density (V_e) and total CI are almost the same for NR/SiO_2/STU composites and NR/SiO_2/TU composites at the same dosage of SiO_2, indicating that these three factors on mechanical properties of NR/SiO_2 composites can be ignored. Two main reasons may be taken into consideration to represent the higher mechanical properties of NR/SiO_2/STU composites. First, as depicts in section 3.3. and Figure 5, the modified effect of STU gives rise to a fine-dispersion structure of SiO_2 in the NR matrix, leading to the small-size effect and less defects in the interphase of NR matrix and SiO_2 particles [7]. Second, the mechanical properties are found to be affected strongly by the entanglement, maybe the predominant reason, between the silane chain and NR matrix at the interfacial region, as illuminates in Figure 9. As described above, STU molecular chain, more exactly the silane chain, can graft to the surface of SiO_2 particles by the reactions between the silanol groups and hydroxyl groups of SiO_2 under heating. According to the theory similar molecules dissolve mutually, the silane chain can dissolve in the NR matrix, as in Figure 9a, leading to entanglement between these two molecular chains

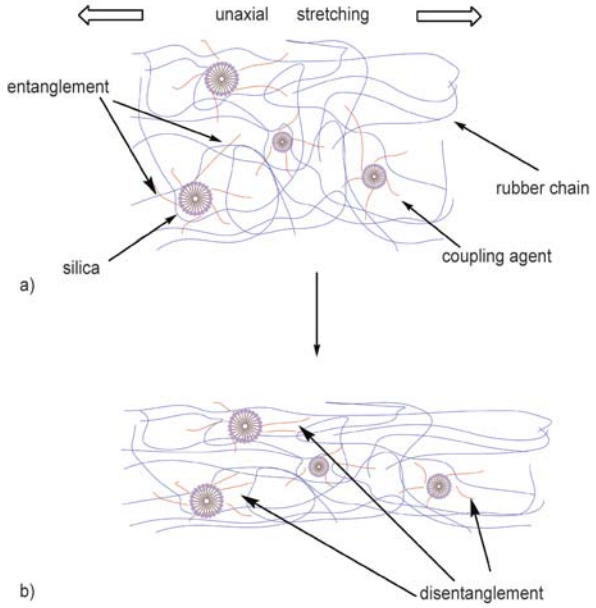

Figure 9. The reinforcement mechanism of STU modified SiO_2 in the NR/SiO_2/STU composites: before stretching (a) and after stretching (b)

at the interfacial region. When an exerted stress is applied to the matrix, the stress runs along the rubber chain, the reinforcement effect of the formed interfacial region becomes more effective to influence the modulus of NR/SiO_2/STU composites, leading to a much higher 400% modulus in the NR/SiO_2/STU composites than that of NR/SiO_2/TU composites at the same addition of SiO_2. As in Figure 9b, when the exerted stress continues to increase, the deformation of 'rubber depletion layer' (often a few nm distances away or larger [7, 25]) surrounding SiO_2 particles would develop [7]. If there are no interactions between NR matrix and SiO_2 particles, decohesion would happen at the interfacial region, following by a catastrophic breakage to the composites under a low tensile strength, like the NR/SiO_2/TU composites. On the other hand, when an entanglement exists in the interfacial region, like NR/SiO_2/STU composites, the stress will pass from NR molecular chains to the filler effectively before disentanglement happens. At the same time, the NR main chains can slip on the SiO_2 particles surface with the help of silane chains, allowing the network to relax to a more perfect regime and changing the local stress condition by means of stress homogenized distribution. These will lead to a much higher 400% modulus and tensile strength in the composites, like STU-SiO_2-30, before disentanglement.

4. Conclusions

Vulcanization property and structure-property relationship of NR/SiO_2 composites modified by a novel multi-functional rubber agent, STU, are explored thoroughly. From the IR and XPS spectra, STU can graft to the surface of SiO_2 under heating, reducing the block vulcanization effect of SiO_2 for rubber vulcanization due to the reduction in the physical adsorption of SiO_2 particles to rubber agents. From the graphs of TEM, STU can facilitate a fine-dispersed structure in the rubber matrix without any connectivity of SiO_2 particles, whereas, for NR/SiO_2 composites without modification, serious aggregation of SiO_2 particles is found. Moreover, the strain-induced crystallization at the stretching ratio of 4 and the crosslinking densities of NR/SiO_2 composites are almost the same at the same dosage of SiO_2. However, the 400% modulus and tensile strength of NR/SiO_2/STU composites are much higher than that of NR/SiO_2/TU composites. Finally, a structure-property relationship of NR/SiO_2/STU composites is

proposed that the silane chain of STU can entangle with NR molecular chains to form an interfacial region. When an exerted stress is applied to the matrix, the stress runs along the rubber chain, the reinforcement effect of the formed interfacial region became more effective to the mechanical properties of NR/SiO_2/STU composites.

Acknowledgements

The authors gratefully acknowledge the financial support from Guangdong Province Joint Funds of the National Natural Science Foundation of China (No. U1134005) and The National Natural Science Funds of China (No.51303026) and Strategic new industry core technology research project of Guangdong Province (2012A090100017).

References

[1] Xiong L., Liang H., Wang R., Chen L.: A novel route for the synthesis of poly(2-hydroxyethyl methacrylate-co-methyl methacrylate) grafted titania nanoparticles via ATRP. Journal of Polymer Research, **18**, 1017–1021 (2011).
DOI: 10.1007/s10965-010-9502-5

[2] Peng H., Liu L., Luo Y., Hong H., Jia D.: Synthesis and characterization of 3-benzothiazolthio-1-propyltriethoxylsilane and its reinforcement for styrene–butadiene rubber/silica composites. Journal of Applied Polymer Science, **112**, 1967–1973 (2009).
DOI: 10.1002/app.29634

[3] Peng H., Liu L., Luo Y., Jia D., Fu W.: Novel blocked mercaptosilane (3-propionylthio-1-propyltrimethoxylsilane) for natural rubber/silica composite reinforcement in various curing systems. e-Polymers, **8**, 1190–1198 (2008).
DOI: 10.1515/epoly.2008.8.1.1190

[4] Murakami K., Iio S., Ikeda Y., Ito H., Tosaka M., Kohjiya S.: Effect of silane-coupling agent on natural rubber filled with silica generated *in situ*. Journal of Materials Science, **38**, 1447–1455 (2003).
DOI: 10.1023/A:1022908211748

[5] Yun S. H., Cho D., Kim J., Lim S., Lee G-W., Park M., Lee S-S.: Effect of silane coupling agents with different organo-functional groups on the interfacial shear strength of glass fiber/nylon 6 composites. Journal of Materials Science Letters, **22**, 1591–1594 (2003).
DOI: 10.1023/A:1026384408153

[6] Jouault N., Vallat P., Dalmas F., Said S., Jestin J., Boué F.: Well-dispersed fractal aggregates as filler in polymer–silica nanocomposites: Long-range effects in rheology. Macromolecules, **42**, 2031–2040 (2009).
DOI: 10.1021/ma801908u

[7] Yang S., Liu L., Jia Z., Jia D., Luo Y.: Structure and mechanical properties of rare-earth complex La-GDTC modified silica/SBR composites. Polymer, **52**, 2701–2710 (2011).
DOI: 10.1016/j.polymer.2011.04.015

[8] Peng H., Liu L., Luo Y., Wang X., Jia D.: Effect of 3-propionylthio-1-propyltrimethoxylsilane on structure, mechanical, and dynamic mechanical properties of NR/silica composites. Polymer Composites, **30**, 955–961 (2009).
DOI: 10.1002/pc.20640

[9] Nakamura Y., Honda H., Harada A., Fujii S., Nagata K.: Mechanical properties of silane-treated, silica-particle-filled polyisoprene rubber composites: Effects of the loading amount and alkoxy group numbers of a silane coupling agent containing mercapto groups. Journal of Applied Polymer Science, **113**, 1507–1514 (2009).
DOI: 10.1002/app.30155

[10] Choi S-S.: Improvement of properties of silica-filled natural rubber compounds using polychloroprene. Journal of Applied Polymer Science, **83**, 2609–2616 (2002).
DOI: 10.1002/app.10201

[11] González L., Rodríguez A., Del Campo A., Marcos-Fernández A.: Crosslink reaction of natural rubber with thiuram sulphur donors in the presence of a thiuram monosulfide. Journal of Applied Polymer Science, **85**, 491–499 (2002).
DOI: 10.1002/app.10438

[12] Susamma A. P., Mini V. T. E., Kuriakose A. P.: Studies on novel binary accelerator system in sulfur vulcanization of natural rubber. Journal of Applied Polymer Science, **79**, 1–8 (2001).
DOI: 10.1002/1097-4628(20010103)79:1<1::AID-APP10>3.0.CO;2-V

[13] Susamma A. P., Claramma N. M., Nair A. B., Kuriakose A. P.: New binary systems containing TMTD-amidino phenyl thiourea and CBS–amidinophenyl thiourea for the vulcanization and rheological behavior of natural rubber latex. Journal of Applied Polymer Science, **115**, 2310–2316 (2010).
DOI: 10.1002/app.31360

[14] Aprem A. S., Joseph K., Mathew T., Volker A., Sabu T.: Studies on accelerated sulphur vulcanization of natural rubber using 1-phenyl-2, 4-dithiobiuret/tertiary butyl benzothiazole sulphenamide. European Polymer Journal, **39**, 1451–1460 (2003).
DOI: 10.1016/S0014-3057(02)00382-8

[15] Kurien M., Kuriakose A. P.: Studies on sulphur vulcanisation of natural rubber using amidino thiourea. Plastics, Rubber and Composites, **30**, 263–269 (2001).
DOI: 10.1179/146580101101541688

[16] Cauzzi D., Costa M., Cucci N., Graiff C., Grandi F., Predieri G., Tiripicchio A., Zanoni R.: Pd(II) and Rh(I) chelate complexes of the bidentate phosphino–thiourea ligand $PhNHC(S)NHCH_2CH_2PPh_2$: Structural properties and activity in homogeneous and hybrid catalysis. Journal of Organometallic Chemistry, **593–594**, 431–444 (2000).
DOI: 10.1016/S0022-328X(99)00615-4

[17] Angelova D., Armelao L., Gross S., Kickelbick G., Seraglia R., Tondello E., Trimmel G., Venzo A.: Investigation of thiourea-silanes as viable precursors for the sol–gel synthesis of composites containing Zn–S complexes. Applied Surface Science, **226**, 144–148 (2004).
DOI: 10.1016/j.apsusc.2003.11.014

[18] Angelova D., Armelao L., Barison S., Fabrizio M., Gross S., Sassi A., Seraglia R., Tondello E., Trimmel G., Venzo A.: Sol–gel synthesis of Zn-thiourea-SiO_2 thin films from $(EtO)_3Si(CH_2)_3NHC(=S)NHPh$ as molecular precursor. Solid State Sciences, **6**, 1287–1294 (2004).
DOI: 10.1016/j.solidstatesciences.2004.06.007

[19] Flory P. J.: Statistical mechanics of swelling of network structures. The Journal of Chemical Physics, **18**, 108–111 (1950).
DOI: 10.1063/1.1747424

[20] Yang S., Liu L., Jia Z., Jia D., Luo Y., Liu Y.: Studies on the influence of lanthanum glutamic dithiocarbamate on the interfacial reinforncement of SBR/SiO_2 composites by swelling equilibrium test. Acta Polymerica Sinica, **52**, 709–719 (2011).
DOI: 10.3724/SP.J.1105.2011.10184

[21] Yang S. Y., Jia Z. X., Liu L., Fu W. W., Jia D. M., Luo Y. F.: New insight into the vulcanization mechanism of novel binary accelerators for natural rubber. Chinese Journal of Polymer Science, in press (2014).

[22] Yang S., Liu L., Jia Z., Jia D., Luo Y.: Study on the curing properties of SBR/La-GDTC/SiO_2 composites. Journal of Rare Earths, **29**, 444–453 (2011).
DOI: 10.1016/S1002-0721(10)60477-2

[23] Yatsuyanagi F., Suzuki N., Ito M., Kaidou H.: Effects of surface chemistry of silica particles on the mechanical properties of silica filled styrene–butadiene rubber systems. Polymer Journal, **34**, 332–339 (2002).
DOI: 10.1295/polymj.34.332

[24] Suzuki N., Yatsuyanagi F., Ito M., Kaidou H.: Effects of surface chemistry of silica particles on secondary structure and tensile properties of silica-filled rubber systems. Journal of Applied Polymer Science, **86**, 1622–1629 (2002).
DOI: 10.1002/app.11050

[25] Starr F. W., Schrøder T. B., Glotzer S. C.: Molecular dynamics simulation of a polymer melt with a nanoscopic particle. Macromolecules, **35**, 4481–4492 (2002).
DOI: 10.1021/ma010626p